DEVELOPMENT OF A BEAM LOSS MONITOR SYSTEM FOR THE LCLS UNDULATOR BEAMLINE*

W. Berg#, J. C. Dooling, A. Pietryla, and B.-X. Yang, Advanced Photon Source,
Argonne National Laboratory, Argonne, IL 60439 USA
H.-D. Nuhn, Linac Coherent Light Source, Stanford Linear Accelerator Center,
Menlo Park, CA 94025 USA

Abstract

A beam loss monitor (BLM) system based on the detection of Cerenkov radiation has been developed at the Advanced Photon Source (APS) for the Linear Coherent Light Source (LCLS) free-electron laser (FEL). The electron beam will vary in energy from 4.6 to 13.6 GeV with a bunch charge of 0.2 to 1.0 nC and a maximum repetition rate of 120 Hz. In order to limit radiation-induced demagnetization of the undulator permanent magnets, the BLM will provide beam-loss threshold detection as part of the Machine Protection System (MPS). The detector incorporates a large-volume (30 cm^3) fused-silica Cerenkov radiator coupled to a photo-multiplier tube (PMT). The output of the PMT is conditioned locally by a charge amplifier and then digitized at the front end of the MPS electronics. During commissioning, the device will be calibrated by inserting a 1-micron aluminum foil into the beam, upstream of the undulator magnets. Tests of a prototype BLM system showed that the detector and electronics are functional. Initial results from computer simulations support the proposed calibration scheme and indicate of the need for a dense population of BLM devices.

INTRODUCTION

APS is developing a beam loss monitor detector as a component of the LCLS Machine Protection System. The BLM is intended to protect the FEL undulator magnets from potential damage resulting from localized and distributed electron beam losses. Detection of a loss event above threshold will limit the beam pulse rate. A secondary usage of the BLM system is to track and archive the radiation dose. The data will be analyzed for correlation to any observed demagnetization or damage in the undulator magnets.

Initially, five detector modules will be distributed throughout the length of the 33 undulator magnets. Calibration of the system will be based on computer simulation using MARS [1, 2] and empirically verified during machine commissioning. Some of the relevant specifications of the electron beam are listed in Table 1.

SYSTEM OVERVIEW

Electron beam loss is measured by collecting Cerenkov radiation generated in a quartz radiator from a high-energy electron shower. The Cerenkov light propagates through the radiator to the UV glass entrance window (185-850 nm) of a single PMT for detection. The PMT output is conditioned locally by an interface module (IM) incorporating a charge amplifier. The amplifier integrates the PMT charge output pulse and converts the signal to a voltage pulse. The output of the amplifier is transmitted over a coaxial line to the MPS instrumentation racks, where signal filtering and a/d conversion is performed. Further signal processing, distribution, threshold detection, and system validation is handled by the MPS.

Table 1: Electron Beam Specifications

Beam Parameter	Value
Max. repetition rate	120 Hz
Beam charge	0.2 - 1.0 nC
Normalized emittance	2.0 - 3.0 μm rad
Beam energy	4.6 - 13.6 GeV
FWHM bunch duration	0.25 - 0.48 ps

BEAM LOSS DETECTOR

The detector design shown in Fig 1 is conceptually derived from a design for the PEP II B-Factory at SLAC [3]. A quartz Cerenkov radiator was chosen over conventional scintillation materials for better immunity to scintillation effects from the high-power x-ray beam emanating from the undulator. The radiator is cut from a single boule of synthetic crystalline quartz. Military-grade fused silica (MIL-G-174B) is used to limit impurities that may result in premature browning of the material from radiation exposure. The tuning fork geometry was chosen so the radiator would cover the surface area of the

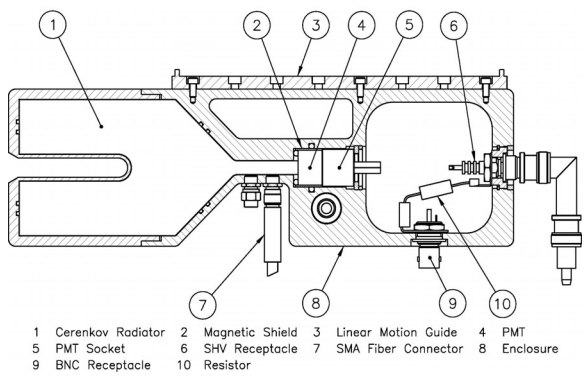

Figure 1: Cross section view of the BLM detector configuration with the component call outs.

*Work supported by U.S. DOE, Office of Science, Office of Basic Energy Sciences, under contract number DE-AC02-06CHI11357.
#berg@aps.anl.gov

undulator pole pieces and still deliver the Cerenkov light to a single PMT. The raw substrate is water-jet rough cut, flame polished, annealed, and lap polished to the final surface figure before plating with an aluminum reflector and protective overcoat.

The detector can be positionally configured to remain at the static home location or to track with the undulator's horizontal motion. This change is accomplished by relocating a capture screw to the undulator field shunt end plate. The BLM housing is mounted to a linear bearing to provide the 100 mm of stroke required. This configuration is intended for when the detector is operated as a dosimeter for tracking exposure levels to the adjacent undulator magnet [4].

SIGNAL CONDITIONING

The BLM interface module (IM) is designed to provide the interface between the PMT and the LCLS MPS link node chassis [5]. The interface electronics are housed in an RFI enclosure located in the tunnel, below the girder. The IM provides three functions: PMT high voltage (HV) supply, signal conditioning, and heartbeat circuit. The interface signals between the IM and the link node chassis are carried by an individually shielded twisted pair cable harness (see Figure 2). The conditioned signal is transported to the link node chassis via 300' of low-loss LMR coaxial cable.

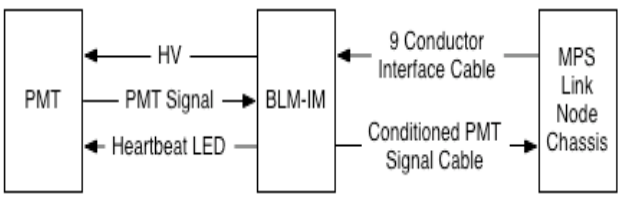

Figure 2: System-level block diagram.

The high-voltage circuit for the PMT is an Emco CA10N [6] module with an output ranging from 0 V to 1000 V. The HV output is set by a 0- to 5-V control signal. The output signal of the PMT is a negative current pulse, approximately 1.8 ns wide, whose integrated charge is proportional to the loss detected. A charge-sensitive amplifier, Cremat CR-112 [7], will integrate this current pulse, providing an output voltage pulse amplitude proportional to the charge. The charge amplifier selected has a decay time constant of 50 µs with an output ranging from 0-1.5 V when terminated with 50 Ω.

The heartbeat signal is a 120-Hz optical pulse sent over a short fiber bundle to the PMT before each beam pulse. The resulting PMT signal is then processed and compared to a fixed threshold. If the heartbeat is not detected, the MPS system will inhibit beam.

Bench testing of the heartbeat circuit was performed to optimize its signal. The heartbeat pulse should be detected over a PMT voltage range of –400- to –900 V representing a large dynamic range (~ 48 dB) for the PMT output. A nominal pulse width of 600 ns allows the heartbeat pulse to be detected when the PMT is operating at –400 V but the charge amplifier output is saturated when operating at –900 V. A choice of a pulse width between 200 ns and 1000 ns is provided.

TEST AND CALIBRATION

A prototype of the beam loss monitor has been constructed with a small quartz Cerenkov radiator block (~ 1.0 cm^3) and tested using stored electron beam in the APS storage ring. The radiator was mounted in 9-ID, approximately 13 mm above the beam and 85 cm from the entrance of the chamber. For stored beams, most of the electrons are lost through Touschek scattering and strike the entrance of ID chambers one electron at a time. The charge amplifier output was sent to an Amptek digital pulse processor/multichannel analyzer (MCA PX4) [8] to analyze the amplitudes of these step pulses and to make the data set into a histogram, as shown in Fig. 3 below.

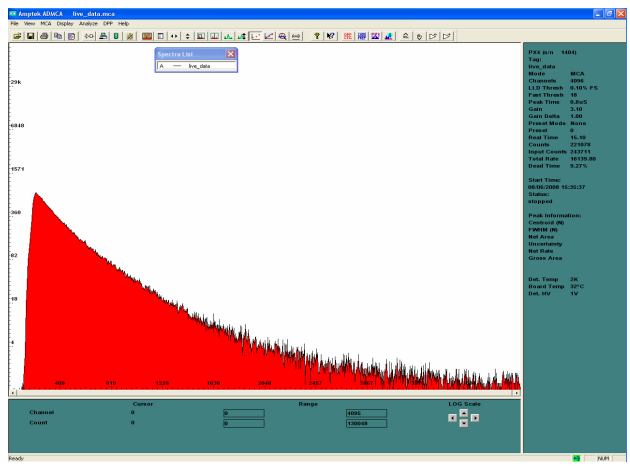

Figure 3: Loss monitor spectrum of stored beam.

Table 2 shows the instrument settings and derived MCA calibration of 10.5 fC/channel. The first moment for the MCA spectrum,

$$Q(N_o) = \sum_{N_o}^{N} n f_n \,, \qquad (1)$$

is the total PMT charge collected during the experiment, where N=4096, f_n is the number events in channel n, and N_o is the cutoff channel. Using the well-behaved portion of the spectrum (N_o>400), the Q (N_o) is extrapolated back to channel 0 to recover the low-energy contribution. This procedure corrects for the effect of the finite-discriminator level and yields an integrated charge of 7.6 µC. Combining this result with the 40-c/s count rate of the existing APS Cerenkov detector [9] and the 9-fC/c calibration of the detector, we arrive at the sensitivity of the LCLS-BLM prototype detector as

$$Q_{\text{LCLS-BLM-Prototype-S9}} = 1.4\times10^{5} Q_{\text{Loss-7GeV-S9}} \,. \qquad (2)$$

These tests not only validate the detector and electronics with the electron beam, but also produce an absolute calibration that can be used to validate the computer simulations performed for these detectors. This calibration has an estimated error of a factor of two.

Table 2: Calibration of LCLS BLM Prototype

Quantity	Values
MCA input sensitivity -MCA preamplifier gain = 3.1 -MCA digitizer full scale = 1.00 V -MCA histogram width = 4095 channel	78.8 μV/channel
CA-MCA input charge sensitivity -Charge amplifier gain = 7.5 V/nC	10.5 fC/channel
Integrated charge (after corrections) -Total charge sum = 4.6 μC -Extrapolation correction of discriminator cutoff leads to 6.9 μC -Dead time = 9.27%	7.6 μC
Lost electron beam charge -APS Cherenkov detector rate = 40 c/s -Cherenkov detector calibration = 9.1 fC/c -Total acquisition time = 15 seconds	5.5 pC
Loss monitor sensitivity this test	1.4×10^5

BEAM-LOSS SIMULATIONS

Monte Carlo simulations of the beam losses and detector signals in both the LCLS undulator and in the APS test site are being performed using the program MARS [1, 2]. In the first case studied, a 1-μm Al foil was used as the scatterer at LCLS OTR-33 station. Beam transport downstream of the foil includes quadrupole magnets and a collimator, with a beam aperture of (0.86 cm × 0.43 cm).

Figure 4 shows the calculated high-energy electron fluence in the LCLS-BLM radiators along the undulators. The fluence is expected to be proportional to the detector signal. When all quads are off, the beam loss can be used to calibrate the monitors. When all quads are on, simulation show a possible axial loss distribution during FEL operations. Unlike the field-free case, the radiation dose can be localized to within one or two undulators. Hence, a sparse distribution of BLM detectors may not be sufficient to measure the beam losses for realistic loss scenarios. Figure 5 shows the calculated electron fluence in the undulator magnets, which are expected to correlate with damage to the undulators. A comparison of Figs. 4 and 5 shows that the signal level of the BLM is correlated with the dose rate in nearby undulators, but is not strictly proportional to it. We also note that the magnetic lattice transports most of the scattered electrons out of the undulator chamber and the dose rate in the undulator is 10- to 100-fold lower than that estimated from the field-free calculation. Model calculations for the test geometry at the APS are in progress and will be reported elsewhere.

CONCLUSIONS

Installation of the BLM hardware will take place this coming fall with commissioning to follow during the first quarter of 2009. Initially, the undulator magnets will not be installed until the machine is tuned and the undulator system components are tested. At the conclusion of this first phase of commissioning in March 2009, the undulator magnets will be installed, and the LCLS will begin generating x-rays. The authors would like to acknowledge our many collaborators at SLAC and our support personnel at ANL for their in-depth input and discussions.

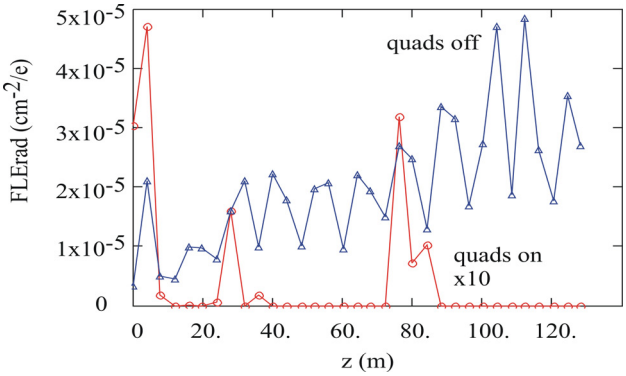

Figure 4: Electron fluence per incident electron in the LCLS BLM radiators with and without quadrupole fields.

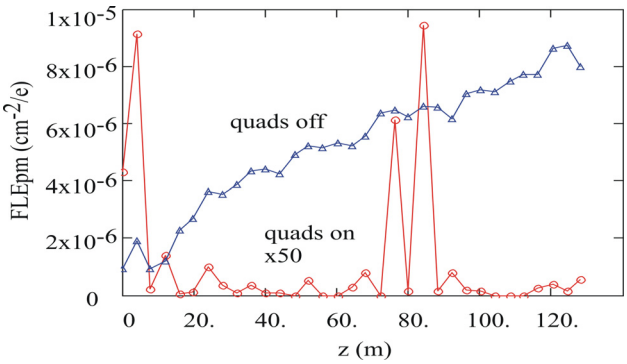

Figure 5: Electron fluence per incident electron in the LCLS undulators with and without quadrupole fields.

REFERENCES

[1] N. V. Mokhov and S. I. Striganov, "Mars15 overview," Technical Report Fermilab-Conf-07/008-AD, 2007.
[2] N. V. Mokhov et al., AIP Conf. Proc. 769, 1618-1623 (2004).
[3] A. Fisher et al., AIP Conf. Proc. 390, 248-256 (1996).
[4] H.-D. Nuhn, Undulator Beam Loss Monitor, LCLS PRD 1.4-005-r0, September 2007
[5] S. Norum, LCLS Machine Protection System, ESD 1.1-315-r1, January 2007.
[6] Emco High Voltage Corporation; http://www.emcohighvoltage.com
[7] Cremat, Inc.; http://cremat.com
[8] Amptek digital pulse processor PX4 datasheet; http://www.amptek.com/px4.html
[9] A. Pietryla et al., Proc. of PAC2001; Chicago, IL, 1622-1624 (2001); http://www.JACoW.org.